

Quantifying the impacts of future gravitational-wave data on constraining interacting dark energy

Hai-Li Li,¹ Dong-Ze He,¹ Jing-Fei Zhang,¹ and Xin Zhang^{*1, 2, 3, †}

¹*Department of Physics, College of Sciences, Northeastern University, Shenyang 110819, China*

²*Ministry of Education's Key Laboratory of Data Analytics and Optimization for Smart Industry, Northeastern University, Shenyang 110819, China*

³*Center for High Energy Physics, Peking University, Beijing 100080, China*

(Dated: May 6, 2022)

In this work, we investigate the impacts of the future gravitational-wave (GW) standard siren observation by the Einstein Telescope (ET) on constraining the interacting dark energy (IDE) models. We simulate 1000 GW events in the redshift range $0 \lesssim z \lesssim 5$ based on the 10-year observation of the ET. We combine the simulated GW data with the current mainstream cosmological electromagnetic observations including the cosmic microwave background (CMB) anisotropies observation, the baryon acoustic oscillations (BAO), and the type Ia supernovae (SN) observation (Pantheon compilation) to constrain the IDE models. We consider two typical IDE models, i.e., the Λ CDM model and Iw CDM model, in the context of a perturbed universe. To avoid the large-scale instability problem for IDE models, we apply the parameterized post-Friedmann (PPF) approach to do the analysis. We find that the addition of GW standard siren data could significantly improve the constraint accuracies on most of the cosmological parameters (e.g., H_0 , w , and Ω_m). For the coupling constant β , the absolute constraint errors could also be slightly improved when adding the GW data in the cosmological fit.

I. INTRODUCTION

The accelerated expansion of Universe, discovered by the observations of type Ia supernovae [1, 2] and further confirmed by the observations of cosmic microwave background [3, 4] and large scale structure [5, 6], has become a fact. In order to explain the cosmic acceleration, the concept of “dark energy”, which is an exotic form of energy with negative pressure and provides repulsive force, has been proposed [7–15]. At present, dark energy (DE) occupies about 68% of the total energy density of cosmos, dominating the evolution of our current universe significantly.

The cosmological constant Λ , proposed by Einstein in 1917, has always been regarded as the simplest candidate of DE until now. The combination of cosmological constant Λ (or vacuum energy) and cold dark matter (CDM) constitute a concordant cosmological prototype, which is also called the Λ CDM model. The equation of state (EoS) parameter of vacuum energy is $w_\Lambda \equiv p_\Lambda/\rho_\Lambda = -1$. Although the Λ CDM model is in excellent agreement with current cosmological observations with the least parameters [16], the cosmological constant Λ has always been bothered by some severe theoretical puzzles, such as the “fine-tuning” and “cosmic coincidence” problems [17, 18]. Thus, it is hard to say that the cosmological constant model with only six primary parameters is the final scenario of our universe, which implies that the Λ CDM model is necessary to be further extended and some new physics maybe exist in the extensions.

To extend the Λ CDM cosmology on the aspect of DE, there are mainly two possible theoretical orientations, i.e., dynamical dark energy and modified gravity (MG) theories. If Einstein’s general relativity (GR) is valid on all the scales of Universe, an alternative proposal of Λ is dynamical dark energy, which suggests that the energy form with negative pressure can be provided by a spatially homogeneous scalar field evolving slowly down a proper potential, dubbed quintessence. On the other hand, if GR could break down on the cosmological scales, some models of MG can mimic the “effective dark energy” at the cosmological background level to explain the cosmic accelerated expansion. In general, a dynamical DE model, compared to the cosmological constant, can yield a different expansion history of the universe but a similar growth history of structure. On the contrary, the MG models can yield a similar expansion history but a quite different structure growth history. Discriminating the scenarios of dynamical DE and MG has become one of the most critical issues in modern cosmology.

However, it must be stressed out that there is another important theoretical possibility that dark energy and dark matter can directly interact with each other, through mediating some unknown scalar field degrees of freedom, also called “the fifth force”. Inspired by this possibility, a large number of models featuring the interactions between dark matter and dark energy have been constructed and researched [19–98]. Although the interaction between dark matter and dark energy is mild, we still cannot exclude it within 1σ confidence region [99–106]. What is important is that the models of interacting dark energy can successfully solve (or alleviate) the fine-tuning and coincidence problems through the attractor solution. Furthermore, the interaction between dark matter and dark energy not only can alleviate the tension in

*Corresponding author

†Electronic address: zhangxin@mail.neu.edu.cn

the values of Hubble constant H_0 originated from its local and global measurements [107], but also can explain the excess amount of 21 cm absorption signal around the redshift $z \sim 17$ detected by the Experiment to Detect the Global Epoch of Reionization Signature (EDGES) [98, 108, 109]. Thus, the research on the interacting dark energy model is expected to be importantly significant and valuable.

Currently, the major cosmological probes include the cosmic microwave background (CMB) anisotropies, baryon acoustic oscillations (BAO), type Ia supernovae (SN), direct determination of the Hubble constant (H_0), weak gravitational lensing (WL), redshift space distortions (RSD) etc. Some important cosmological parameters have been precisely measured by the combination of these electromagnetic (EM) probes. But for the parameters beyond the standard model, such as the EOS of dark energy, the sterile neutrino mass, the tensor-to-scalar ratio and so forth, we still cannot measure them accurately up to now. In fact, there are strong degeneracies between these parameters, and some conflicts also exist among various observations. The reason for the situation is that, the current observation are still not accurate enough so that we can not precisely measure the cosmological parameters beyond the standard model. In order to better constrain these parameters, we also need some new cosmological probes other than the traditional optical cosmological probes.

As proposed by Schutz in 1986 [110] and subsequently discussed by Holz and Hughes [111], the observations of the gravitation wave (GW) can be used as the *standard sirens* in cosmology. The detection of GW event GW170817 from the merge of binary neutron star (BNS) and its EM counterpart GRB170817A has pronounced the arrival of the multi-messenger astronomy era. With the help of the multi-messenger observation, we can measure the absolute luminosity distance d_L of the source from the gravitational wave signal as well as the redshift z from the electromagnetic counterparts. Then, we can establish a true distance-redshift relation which can be used to infer the expansion history of universe and constrain the cosmological parameters such as Hubble constant [112]. The main advantage of the standard siren method is that it avoids using the cosmic distance ladder. Therefore, the future GW standard sirens would become a promising new cosmological probe, and would play a significant role in the cosmological parameter measurements.

Actually, in the near future, a planned third-generation ground-based GW detector, the Einstein Telescope (ET), will be brought into operation [113]. This impressive equipment will hold 10 km-long arms and three detectors. Compared with the advanced LIGO, it has a much wider detection frequency range and a much better detection sensitivity. Thus, there will be much more BNS events in much deeper redshifts detected by ET. As a conservative estimation, at least 1000 useful standard siren events data will be observed with ET's ten years opera-

tion [114]. In some previous works [114–124], the authors have already utilized the GW standard siren observation to estimate the cosmological parameters in many various cosmological models. For example, in Ref. [114] the authors have investigated the capability of future GW standard siren observation on improving the parameter estimation in cosmology and breaking the parameter degeneracies formed in traditional EM observations. Taking ET as an example, they simulated 1000 events data based on the ten years observation and find that, the simulated GW data could largely break the parameter degeneracy in Λ CDM model as well as w CDM model, significantly improving the parameter constraints in the cosmological fit. In Ref. [121], the authors have also investigated the Chevallier-Polarski-Linder (CPL) model, α dark energy (α DE) model, generalized Chaplygin gas (GCG) model and new generalized Chaplygin gas (NGCG) model with the simulated GW standard siren data, and GW data could also improve the constraints on the cosmological parameters for all these DE models. Likewise, the similar conclusion was also obtained for the holographic dark energy (HDE) models in Ref. [117].

As for the interacting dark energy (IDE) models, Ref. [119] has recently investigated how the future GW data could help improve the limits on the parameters in two specific Λ CDM models (with a positive coupling), finding that the addition of GW data to the CMB data can reduce the current uncertainty by a factor of 5. In this work, we will further explore the impacts of the future GW data on improving the parameter constraints or breaking the parameter degeneracy for extensive IDE models (e.g., Λ CDM model and Iw CDM model). We consider another two cases of energy transfer rate, i.e., $Q = \beta H \rho_c$ and $Q = \beta H_0 \rho_c$, where ρ_c is the energy density of cold dark matter. In order to treat the cosmological perturbation evolution in these models, we employ the parameterized post-Friedmann (PPF) scheme for the IDE scenario [125] to make the calculations. This work will make the analysis of the constraining power of future GW standard siren observation on cosmological parameters more general and complete.

This paper is organized as follows. In Sec. II, we give a brief description of the PPF approach in the interacting dark energy models. In Sec. III, we introduce the current standard cosmological data and briefly describe the method to simulate the gravitational wave data. In Sec. IV, we report the constraint results and make some relevant discussions for them. Conclusion is given in Sec. V.

II. A BRIEF DESCRIPTION OF THE PPF APPROACH FOR THE INTERACTING DARK ENERGY MODELS

If there is a direct, non-gravitational interaction between dark energy and dark matter, we will have the

following energy continuity equations

$$\rho'_{\text{de}} = -3\mathcal{H}(1+w)\rho_{\text{de}} + aQ_{\text{de}}, \quad (1)$$

$$\rho'_c = -3\mathcal{H}\rho_c + aQ_c, \quad Q_{\text{de}} = -Q_c = Q, \quad (2)$$

where ρ_{de} and ρ_c are the energy densities of dark energy and dark matter; a prime is the derivative with respect to the conformal time η ; $\mathcal{H} = a'/a$ is the conformal Hubble expansion rate; a denotes the scale factor; w is the EoS parameter; and Q is the phenomenological interaction term. Generally, the form of Q is assumed to be proportional to the density of dark sectors, and it can include the Hubble parameter H or the Hubble constant H_0 . In this paper, we consider two forms of the interaction term Q , e.g., $Q = \beta H \rho_c$, $Q = \beta H_0 \rho_c$, with β being a dimensionless coupling parameter used to describe the interacting strength between dark energy and dark matter. From Eqs. (1) and (2), we can clearly find that if $\beta > 0$, dark matter would decay into dark energy, and vice versa for $\beta < 0$. Here, $\beta = 0$ denotes no interaction between the two sectors.

The covariant conservation law of the dark sectors can be expressed as

$$\nabla_\nu T_I^{\mu\nu} = Q_I^\mu, \quad \sum_I Q_I^\mu = 0, \quad (3)$$

where $T_I^{\mu\nu}$ is the energy-momentum tensor, and Q_I^μ is the energy-momentum transfer vector. In this paper, we choose $Q_{\text{de}}^\mu = -Q_c^\mu = Qu_c^\mu$, where u_c^μ is the four-velocity of dark matter. The energy-momentum transfer vector Q_I^μ can be split into two parts as

$$Q_I^\mu = a(-Q_I(1+AY) - \delta Q_I Y, [f_I + Q_I(v-B)]Y_i), \quad (4)$$

where δQ_I is the energy transfer perturbation and f_I is the momentum transfer potential of the I fluid. A and B are the scalar metric perturbations. Y is the eigenfunctions of the Laplace operator ($\nabla^2 Y = -k^2 Y$) and Y_i is the covariant derivative ($Y_i = (-k)\nabla_i Y$).

In the interacting dark energy models, we can give the following conservation equations for the I fluid according to Equations (3) and (4),

$$\delta\rho'_I + 3\mathcal{H}(\delta\rho_I + \delta p_I) + (\rho_I + p_I)(kv_I + 3H'_L) = a(\delta Q_I + AQ_I), \quad (5)$$

$$[(\rho_I + p_I)(v_I - B)]' + 4\mathcal{H}(\rho_I + p_I)(v_I - B) - k\delta p_I + \frac{2}{3}kc_K p_I \Pi_I - k(\rho_I + p_I)A = a[Q_I(v - B) + f_I], \quad (6)$$

In the equations above, $\delta\rho_I$ is the energy density perturbation, δp_I is the isotropic pressure perturbation, v_I is the velocity perturbation, and $c_K = 1 - 3K/k^2$ with K being the spatial curvature, and Π_I is the anisotropic stress perturbation.

When considering the interaction between dark matter and dark energy, dark energy is treated as a nonadiabatic fluid and the calculation of δp_{de} is in terms of the adiabatic sound speed and the rest-frame sound speed. Under

such circumstances, the interacting dark energy models will be confused with the problem of large-scale instability. Hence, we should treat the dark energy perturbations under the generalized PPF framework [125]. For clarity, in the following discussion, we will use some new symbols, i.e., $\zeta \equiv H_L$, $\xi \equiv A$, $\rho\Delta \equiv \delta\rho$, $\Delta p \equiv \delta p$, $V \equiv v$, and $\Delta Q_I \equiv \delta Q_I$, to denote the corresponding quantities of the comoving gauge, except the two gauge-independent quantities Π and f_I .

On the large scales, the direct relationship between $V_{\text{de}} - V_T$ and V_T can be established, and it can be parametrized by a function $f_\zeta(a)$ as [126, 127]

$$\lim_{k_H \ll 1} \frac{4\pi G a^2}{\mathcal{H}^2} (\rho_{\text{de}} + p_{\text{de}}) \frac{V_{\text{de}} - V_T}{k_H} = -\frac{1}{3} c_K f_\zeta(a) k_H V_T, \quad (7)$$

where $k_H = k/\mathcal{H}$. The equation of motion for the curvature perturbation ζ on the large scales can be get by combining this equation with Einstein equations,

$$\lim_{k_H \ll 1} \zeta' = \mathcal{H}\xi - \frac{K}{k} V_T + \frac{1}{3} c_K f_\zeta(a) k V_T. \quad (8)$$

On the small scales, one can describe the evolution of curvature perturbation by using Poisson equation, $\Phi = 4\pi G a^2 \Delta_T \rho_T / (k^2 c_K)$, with $\Phi = \zeta + V_T/k_H$. These two limits can be linked by the introduction of a dynamical function Γ ,

$$\Phi + \Gamma = \frac{4\pi G a^2}{k^2 c_K} \Delta_T \rho_T, \quad (9)$$

which is satisfied for all the scales.

Compared with the small-scale Poisson equation, Eq. (9) gives $\Gamma \rightarrow 0$ at $k_H \gg 1$. Combining the derivative of Eq. (9) with the conservation equations and the Einstein equations, the equation of motion for Γ on the large scales can be expressed as follows,

$$\lim_{k_H \ll 1} \Gamma' = S - \mathcal{H}\Gamma, \quad (10)$$

with

$$S = \frac{4\pi G a^2}{k^2} \left\{ [(\rho_{\text{de}} + p_{\text{de}}) - f_\zeta(\rho_T + p_T)] k V_T + \frac{3a}{k_H c_K} [Q_c(V - V_T) + f_c] + \frac{a}{c_K} (\Delta Q_c + \xi Q_c) \right\},$$

where ξ can be obtained from Eq. (6),

$$\xi = -\frac{\Delta p_T - \frac{2}{3} c_K p_T \Pi_T + \frac{a}{k} [Q_c(V - V_T) + f_c]}{\rho_T + p_T}. \quad (11)$$

By the transition scale parameter c_Γ , we can take the equation of motion for Γ on all scales to be [126, 127]

$$(1 + c_\Gamma^2 k_H^2) [\Gamma' + \mathcal{H}\Gamma + c_\Gamma^2 k_H^2 \mathcal{H}\Gamma] = S. \quad (12)$$

From Eq. (12) we can see that in the equation of motion for Γ , all of the perturbation quantities contain only

the matters and without dark energy. So, we can also solve Eq. (12) without using any information related to the dark energy perturbations. As long as we know the evolution of Γ , we can get the energy density and velocity perturbations immediately,

$$\rho_{\text{de}}\Delta_{\text{de}} = -3(\rho_{\text{de}} + p_{\text{de}})\frac{V_{\text{de}} - V_T}{k_H} - \frac{k^2 c_K}{4\pi G a^2}\Gamma, \quad (13)$$

$$V_{\text{de}} - V_T = \frac{-k}{4\pi G a^2(\rho_{\text{de}} + p_{\text{de}})F} \times \left[S - \Gamma' - \mathcal{H}\Gamma + f_\zeta \frac{4\pi G a^2(\rho_T + p_T)}{k} V_T \right], \quad (14)$$

with $F = 1 + 12\pi G a^2(\rho_T + p_T)/(k^2 c_K)$.

III. DATA AND METHOD

In this section we will firstly describe the current observational data we used in this paper, and then introduce the simulated GW data from the Einstein Telescope.

The current observational data sets we used in this work include CMB, BAO and SN. For the CMB data, we use the planck temperature and polarization power spectra of the full range of multipoles [128], which is usually denoted as ‘‘Planck TT, TE, EE+lowTEB’’. For the BAO data, we use the measurements from 6dFGS ($z_{\text{eff}} = 0.106$) [129], SDSS-MGS ($z_{\text{eff}} = 0.15$) [130], and BOSS DR12 ($z_{\text{eff}} = 0.38, 0.51, \text{ and } 0.61$) [131]. For the SN data, we use the latest Pantheon sample, which is comprised of 1048 data points from the Pantheon compilation [132].

Next, we shall introduce the technology to generate the GW standard siren data specifically. Each data point consists of a triple $(z_i, d_L(z_i), \sigma_i)$. z_i is the redshift of the GW source. $d_L(z_i)$ is the luminosity distance at z_i , and σ_i is the error. The simulation method is the same as described in Refs. [114, 133–135]. The GW sources considered in this work are the combination of the black hole-neutron star (BHNS) and the binary neutron star (BNS), both of which are expected to exhibit the after-flows in the electromagnetic (EM) radiation after they emit a burst of GW signals. Thus, BNS and NSBH could be observed as not only an transient EM counterpart but also a GW event. The consideration of NSBH is likely to exert a beneficial effect on the determination of cosmological parameters [134]. But for NSBH, the intrinsic coalescence rates in the local universe ($z = 0$) are expected to be considerably lower than that for BNS as indicated in the Conceptual Design Study of the Einstein Telescope [113] (see Table 2 on Page 31). Thus, for the GW data simulation, we mainly consider the coalescence events of BNS and only consider a small number of NSBH coalescence events. According to the prediction of the Advanced LIGO-Virgo network [136], the ratio between NSBH and BNS is set to be 0.03 so as to make BNS

the majority of GW source, which is also in accordance with Refs. [114, 117, 121, 133, 135].

Then, we can calculate the redshift distribution of the observable sources [134, 135]

$$P(z) \propto \frac{4\pi d_C^2(z)R(z)}{H(z)(1+z)}, \quad (15)$$

where $d_C(z)$ is the comoving distance at the redshift z , and $R(z)$ denotes the redshift evolution of the burst rate that takes the form as [135, 137, 138]

$$R(z) = \begin{cases} 1 + 2z, & z \leq 1, \\ \frac{3}{4}(5 - z), & 1 < z < 5, \\ 0, & z \geq 5. \end{cases} \quad (16)$$

Furthermore, we can get the catalogue of the GW sources by choosing a fiducial model. Theoretically, the fiducial model could be any well motivated cosmological model. In this paper, we take the best-fit interacting dark energy model (i.e., the Λ CDM model and Iw CDM model) constrained by the current observations as the fiducial model to produce the simulated GW data. For the base 6-parameter Λ CDM model, the cosmological parameters are $\{\omega_b, \omega_c, 100\theta_{\text{MC}}, \tau, n_s, \ln(10^{10}A_s)\}$, where $\omega_b = \Omega_b h^2$ and $\omega_c = \Omega_c h^2$ are the present densities of baryons and cold dark matter respectively; θ_{MC} is the ratio between the sound horizon to angular diameter distance at the decoupling epoch; τ is the reionization optical depth; n_s is the scalar spectral index; and A_s is the amplitude of primordial scalar perturbation power spectrum. As an extension of Λ CDM model, the w CDM model has an additional parameter $w = \text{constant}$ relative to the Λ CDM model. Similarly, the $I\Lambda$ CDM model has an additional coupling parameter β relative to the Λ CDM model; the Iw CDM model has an additional coupling parameter β relative to the w CDM model.

The comoving distance $d_C(z)$ can be calculated by the function

$$d_C(z) = \frac{1}{H_0} \int_0^z \frac{dz'}{E(z')}, \quad (17)$$

where $E(z) = H(z)/H_0$ is corresponding to the fiducial model. Therefore, according to the redshift distribution of the GW sources, we can generate a catalog of the GW sources by Eq. (17), which means that the relation between z and d_L can be given for each fiducial model.

Since the GW amplitude depends on the luminosity distance d_L , the information of d_L and σ_{d_L} can be obtained from the amplitude of waveform. The strain $h(t)$ in the GW interferometers can be written as

$$h(t) = F_+(\theta, \phi, \psi)h_+(t) + F_\times(\theta, \phi, \psi)h_\times(t), \quad (18)$$

where the F_+ and the F_\times are the beam pattern functions, ψ is the polarization angle, θ and ϕ are the location of the GW source relative to the GW detector. The antenna

pattern functions of the ET can be written as [134]

$$\begin{aligned} F_+^{(1)}(\theta, \phi, \psi) &= \frac{\sqrt{3}}{2} \left[\frac{1}{2} (1 + \cos^2(\theta)) \cos(2\phi) \cos(2\psi) \right. \\ &\quad \left. - \cos(\theta) \sin(2\phi) \sin(2\psi) \right], \\ F_\times^{(1)}(\theta, \phi, \psi) &= \frac{\sqrt{3}}{2} \left[\frac{1}{2} (1 + \cos^2(\theta)) \cos(2\phi) \sin(2\psi) \right. \\ &\quad \left. + \cos(\theta) \sin(2\phi) \cos(2\psi) \right]. \end{aligned} \quad (19)$$

Obviously, the antenna pattern functions of the other two interferometers can also be calculated from the Eq. (19), due to the three interferometers are placed in an equilateral triangle shape, with the angles with each other being 60° .

Next, we compute the Fourier transform $\mathcal{H}(f)$ of the time domain waveform $h(t)$,

$$\mathcal{H}(f) = \mathcal{A} f^{-7/6} \exp[i(2\pi f t_0 - \pi/4 + 2\psi(f/2) - \varphi_{(2.0)})], \quad (20)$$

Here, \mathcal{A} denotes the Fourier amplitude which can be expressed as

$$\begin{aligned} \mathcal{A} &= \frac{1}{d_L} \sqrt{F_+^2 (1 + \cos^2(\iota))^2 + 4F_\times^2 \cos^2(\iota)} \\ &\quad \times \sqrt{5\pi/96\pi^{-7/6} \mathcal{M}_c^{5/6}}, \end{aligned} \quad (21)$$

where $\mathcal{M}_c = M\eta^{3/5}$ is the ‘‘chirp mass’’ related to the total mass M of the coalescing binary system, m_1 and m_2 are the component masses, and the $\eta = m_1 m_2 / M^2$ is the symmetric mass ratio. The masses of M and \mathcal{M}_c are all the observed quantity, and the relation between the observed mass and the intrinsic mass is $M_{\text{obs}} = (1 + z)M_{\text{int}}$, with the cosmic expansion factor being $(1 + z)$. In Eq. (21), ι denotes the angle of inclination of the binary’s orbital angular momentum with the line of sight. Since the short gamma ray bursts (SGRBs) are strongly beamed, the binaries should be orientated nearly face on (i.e., $\iota \simeq 0$) as implied by the coincidence observations of SGRBs and the maximal inclination is about $\iota = 20^\circ$.

Once the waveform of the GWs is known, the signal-to-noise ratio (SNR) for the network of three independent interferometers can be calculated by

$$\rho = \sqrt{\sum_{i=1}^3 (\rho^{(i)})^2}, \quad (22)$$

where $\rho^{(i)} = \sqrt{\langle \mathcal{H}^{(i)}, \mathcal{H}^{(i)} \rangle}$, and the inner product of the $a(t)$ and $b(t)$ can be defined as

$$\langle a, b \rangle = 4 \int_{f_{\text{lower}}}^{f_{\text{upper}}} \frac{\tilde{a}(f) \tilde{b}^*(f) + \tilde{a}^*(f) \tilde{b}(f)}{2} \frac{df}{S_h(f)}, \quad (23)$$

where a ‘‘ \sim ’’ above the function represents the Fourier transform of the each quantity and $S_h(f)$ is the one-side noise power spectral density. Note that, here, we have

taken the $S_h(f)$ of the ET to be the same as that in Ref. [134].

The Fisher information matrix can be used to estimate the instrumental error on the measurement of d_L ,

$$\sigma_{d_L}^{\text{inst}} \simeq \sqrt{\left\langle \frac{\partial \mathcal{H}}{\partial d_L}, \frac{\partial \mathcal{H}}{\partial d_L} \right\rangle^{-1}}. \quad (24)$$

Because the d_L is independent from other parameters, according to the relation $\mathcal{H} \propto d_L^{-1}$, we can easily get $\sigma_{d_L}^{\text{inst}} \simeq d_L / \rho$. When considering the effect of the inclination angle ι ($0^\circ < \iota < 90^\circ$), we need to add a factor 2 in front of the error, it means that the error should be written as

$$\sigma_{d_L}^{\text{inst}} \simeq \frac{2d_L}{\rho}. \quad (25)$$

In addition, we have to consider a error from the weak lensing which can be expressed as $\sigma_{d_L}^{\text{lens}} = 0.05z d_L$ [135]. Therefore, the total error of the luminosity distance is

$$\begin{aligned} \sigma_{d_L} &= \sqrt{(\sigma_{d_L}^{\text{inst}})^2 + (\sigma_{d_L}^{\text{lens}})^2} \\ &= \sqrt{\left(\frac{2d_L}{\rho}\right)^2 + (0.05z d_L)^2}. \end{aligned} \quad (26)$$

Now, we can generate the catalogue of the GW standard sirens data ($z_i, d_L(z_i), \sigma_i$). In Ref. [135], it pointed out that the sensitivity of at least 1000 GW events is similar to the Planck’s constraining ability. Thus, in this paper, we also simulate 1000 GW standard siren data points which are expected to be detected by the ET in its future 10-year observation.

In order to constrain the cosmological parameters, we will use the Markov chain Monte Carlo (MCMC) method to infer the posterior probability distributions. The procedure is as follows. First, we will use the current data combination of CMB+BAO+SN to constrain the Λ CDM and Iw CDM models, and then we use the obtained best-fit values of the cosmological parameters (except for coupling constant β) to simulate the future GW data; due to the central value of the coupling constant β is around zero, we take the fiducial value as $\beta = 0$ for this parameter. Second, we will add the simulated GW standard sirens data into our analysis and combine with the current cosmological data (CMB+BAO+SN+GW) to constrain the IDE models again, investigating whether the additional GW data can improve the constraints on the parameters of IDE models.

For the amount of simulated GW data points N , the χ^2 function can be written as

$$\chi_{\text{GW}}^2 = \sum_{i=1}^N \left[\frac{\bar{d}_L^i - d_L(\bar{z}_i; \vec{\Omega})}{\bar{\sigma}_{d_L}^i} \right]^2, \quad (27)$$

where \bar{z}_i , \bar{d}_L^i , and $\bar{\sigma}_{d_L}^i$ are the i th redshift, luminosity distance, and error of luminosity distance respectively, and $\vec{\Omega}$ denotes the set of cosmological parameters.

For the combination of the conventional EM observations and the GW standard siren observation, the total χ_{tot}^2 function is

$$\chi_{\text{tot}}^2 = \chi_{\text{CMB}}^2 + \chi_{\text{BAO}}^2 + \chi_{\text{SN}}^2 + \chi_{\text{GW}}^2. \quad (28)$$

IV. RESULTS AND DISCUSSION

In this section, we exhibit the main constraint results in Figs. 1–4, and summarize in Tables I–IV. In Figs. 1–4, the constraint results for the Λ CDM1 model with $Q = \beta H\rho_c$, Λ CDM2 model with $Q = \beta H_0\rho_c$, and Iw CDM1 model with $Q = \beta H\rho_c$, Iw CDM2 model with $Q = \beta H_0\rho_c$ are shown, respectively. In these figures, one-dimensional marginalized posterior distributions and the two-dimensional contours (68.3% and 95.4% confidence level) from CMB+BAO+SN and CMB+BAO+SN+GW are colored by blue and green, respectively. The fit values of the cosmological parameters for the IDE models are given in Tables I and II. The constraint errors of the cosmological parameters are given in Tables III, and the constraint accuracies are given in Tables IV. Here, the error σ is the root-mean-square of σ_+ and σ_- , and for a parameter ξ the accuracy $\varepsilon(\xi)$ can be defined as $\varepsilon(\xi) = \sigma(\xi)/\xi$. For convenience, the data combination “CMB+BAO+SN” is abbreviated as “CBS” in the following.

At first glance in these figures, we can easily find that the addition of GW standard sirens data can tighten the constraint on H_0 and Ω_m significantly (except this case in the Iw CDM2 model with $Q = \beta H_0\rho_c$, which will be discussed in the following), but for the other parameters, the constraints are slightly weak.

The constraint results for the Λ CDM1 model with $Q = \beta H\rho_c$ are shown in Fig. 1. We find that the CBS data provided a 0.95% measurement for H_0 , whereas the combined CBS+GW data provided a 0.32% measurement. For the parameter Ω_m , the CBS data can give a constraint accuracy at 2.66%. When adding the GW data, the constraint accuracy on Ω_m can be improved to 0.95% level with the CBS+GW data. Obviously, both of these two parameters can be constrained more stringent with the help of GW data. Note here that, since central value of the coupling constant β in IDE models is around zero, the relative error for this parameter will be immensely influenced by the statistic fluctuations. Therefore, the absolute error is more reliable for quantifying the improvement of this parameter. The addition of the GW data will tighten the constraint on the coupling constant β , with the absolute error improved from $\sigma(\beta) = 1.2 \times 10^{-3}$ to $\sigma(\beta) = 8.8 \times 10^{-4}$.

The constraint results for the Λ CDM2 model with $Q = \beta H_0\rho_c$ are shown in Fig. 2. For this model, the CBS data can provide a 1.18% measurement for H_0 , while the CBS+GW data can measure H_0 at the 0.49% level. With respect to the parameter Ω_m , the CBS+GW data can give a constraint accuracy on Ω_m at 2.50%, better than

the constraint from CBS data with just a 5.33% accuracy. For the coupling constant β , the result is similar to the case of Λ CDM1 model, and the constraint error could be improved from $\sigma(\beta) = 4.4 \times 10^{-2}$ to $\sigma(\beta) = 3 \times 10^{-2}$ with the addition of GW data.

The results for the Iw CDM1 model with $Q = \beta H\rho_c$ are shown in Fig. 3. From this figure, we find the situation is similar to that of the Λ CDM models. We can see that the CBS data can only provide a 1.23% measurement for H_0 , while the combined CBS+GW data constrain the H_0 with a 0.26% accuracy. As for the measurement of Ω_m , we find that the constraint result of the CBS+GW data is also better than the CBS data. When adding the GW data, the constraint accuracy of Ω_m will be improved from 2.67% to 0.94%. For the parameter w , there is a slight improvement when adding the GW data, with the accuracy enhanced from 3.86% to 2.51%. For coupling parameter β , the constraint error is at the $\sigma(\beta) = 1.5 \times 10^{-3}$ level and $\sigma(\beta) = 1.3 \times 10^{-3}$ in the data combinations CBS and CBS+GW. The improvement in this case is not evident.

Finally, we will investigate the Iw CDM2 model with $Q = \beta H_0\rho_c$, of which the constraint results are shown in Fig. 4. Totally speaking, we find that the constraint accuracy on Ω_m is worse compared with the cases in the above mentioned three models. When adding the GW data, the constraint on Ω_m is at the 5.86% level by the combined CBS+GW data, slightly better than the CBS data with a 7.98% accuracy. In addition, we also find that the CBS data can provide a 1.21% measurement for H_0 , and the combined CBS+GW data provides a 0.59% measurement for H_0 . Similar to the case of Iw CDM1 model with $Q = \beta H\rho_c$, the accuracy of w only has a slight improvement, which is from 7.65% to 6.35%. For the coupling parameter β , when we adding the GW data, the constraint error would slightly decreased, from $\sigma(\beta) = 9.3 \times 10^{-2}$ to $\sigma(\beta) = 7.8 \times 10^{-2}$.

In addition, in order to explore the asymptotic properties of the interaction $Q(z)$, we plot the evolutions of $Q/H_0\rho_{\text{cr}0}$ ($\rho_{\text{cr}0} = 3M_{\text{pl}}^2 H_0^2$ is the present-day critical density of the universe) with 1σ uncertainties for the Λ CDM models in Fig. 5 by using the best-fit results under the data combinations of CMB+BAO+SN and CMB+BAO+SN+GW, which are colored in blue and pink, respectively. We can clearly see that both of the two forms of energy transfer rate Q would become greater with the redshift growth, whereas the case of $Q = \beta H_0\rho_c$ in the Λ CDM2 model would behave more obviously than that of $Q = \beta H\rho_c$ in the Λ CDM1 model. Besides, the interaction terms Q always retain positive with the redshift growth, which implies that dark matter would decay into dark energy in the course of the cosmic evolution.

In summary, for all the IDE models considered in this paper, the future GW standard siren data observed by the ET can indeed improve the constraint accuracies on most of the cosmological parameters, e.g., Ω_m , H_0 , and w . Additionally, for the coupling constant β , when adding the GW data, the constraint error would also be

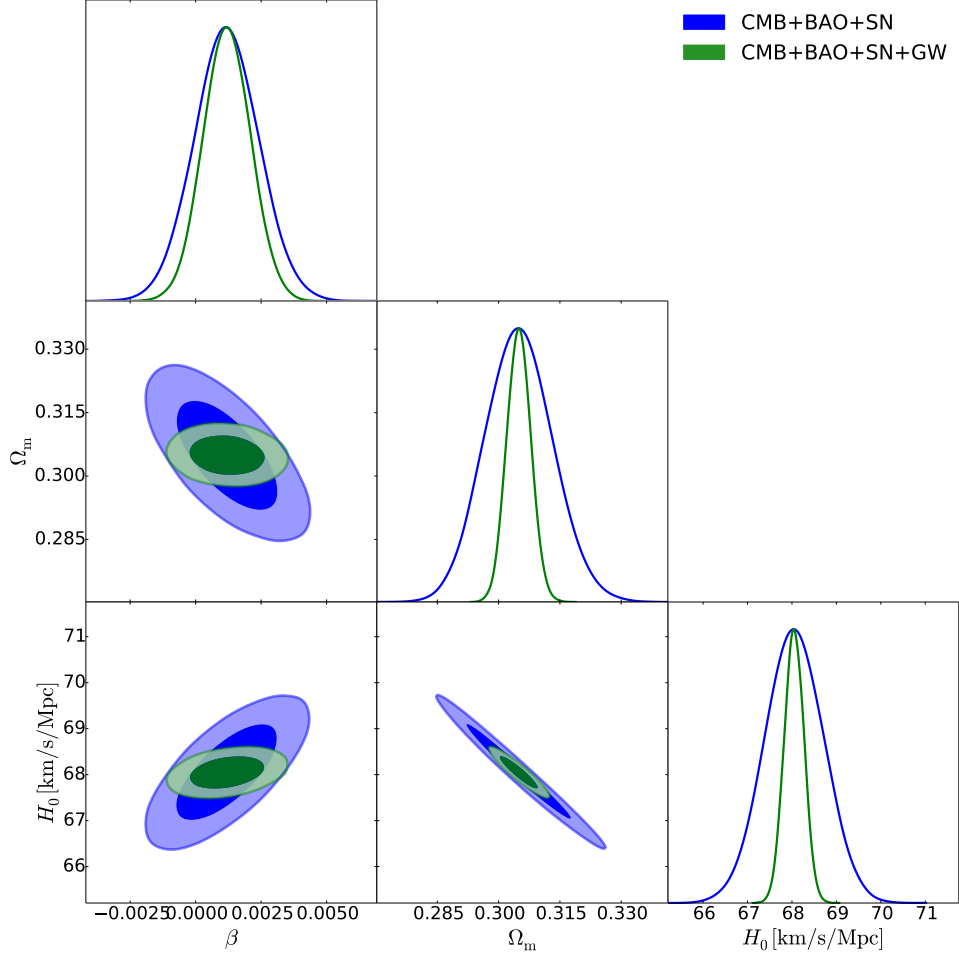


FIG. 1: Observational constraints (68.3% and 95.4% confidence level) on the Λ CDM1 model with $Q = \beta H \rho_c$ by using the CMB+BAO+SN and CMB+BAO+SN+GW data.

TABLE I: Fitting results (68.3% confidence level) for the Λ CDM models using CBS and CBS+GW. Here, CBS stands for CMB+BAO+SN.

Model	I Λ CDM1 ($Q = \beta H \rho_c$)		I Λ CDM2 ($Q = \beta H_0 \rho_c$)	
	CBS	CBS+GW	CBS	CBS+GW
Ω_m	$0.305^{+0.008}_{-0.0081}$	0.305 ± 0.0029	$0.3^{+0.015}_{-0.017}$	$0.3002^{+0.0075}_{-0.0074}$
H_0 [km/s/Mpc]	$68.05^{+0.65}_{-0.64}$	68.05 ± 0.22	68.06 ± 0.8	68.04 ± 0.33
β	0.0012 ± 0.0012	0.0012 ± 0.00088	0.031 ± 0.044	0.031 ± 0.03

TABLE II: Fitting results (68.3% confidence level) for the Iw CDM model using CBS and CBS+GW. Here, CBS stands for CMB+BAO+SN.

Model	Iw CDM1 ($Q = \beta H \rho_c$)		Iw CDM2 ($Q = \beta H_0 \rho_c$)	
	CBS	CBS+GW	CBS	CBS+GW
Ω_m	$0.3073^{+0.0081}_{-0.0082}$	$0.3071^{+0.0028}_{-0.0029}$	$0.332^{+0.025}_{-0.028}$	$0.324^{+0.018}_{-0.02}$
H_0 [km/s/Mpc]	$68.13^{+0.84}_{-0.83}$	68.13 ± 0.18	68 ± 0.82	68.02 ± 0.4
β	-0.0005 ± 0.0015	-0.0005 ± 0.0013	-0.095 ± 0.093	-0.067 ± 0.078
w	-1.036 ± 0.04	-1.036 ± 0.026	$-1.105^{+0.093}_{-0.075}$	$-1.075^{+0.074}_{-0.062}$

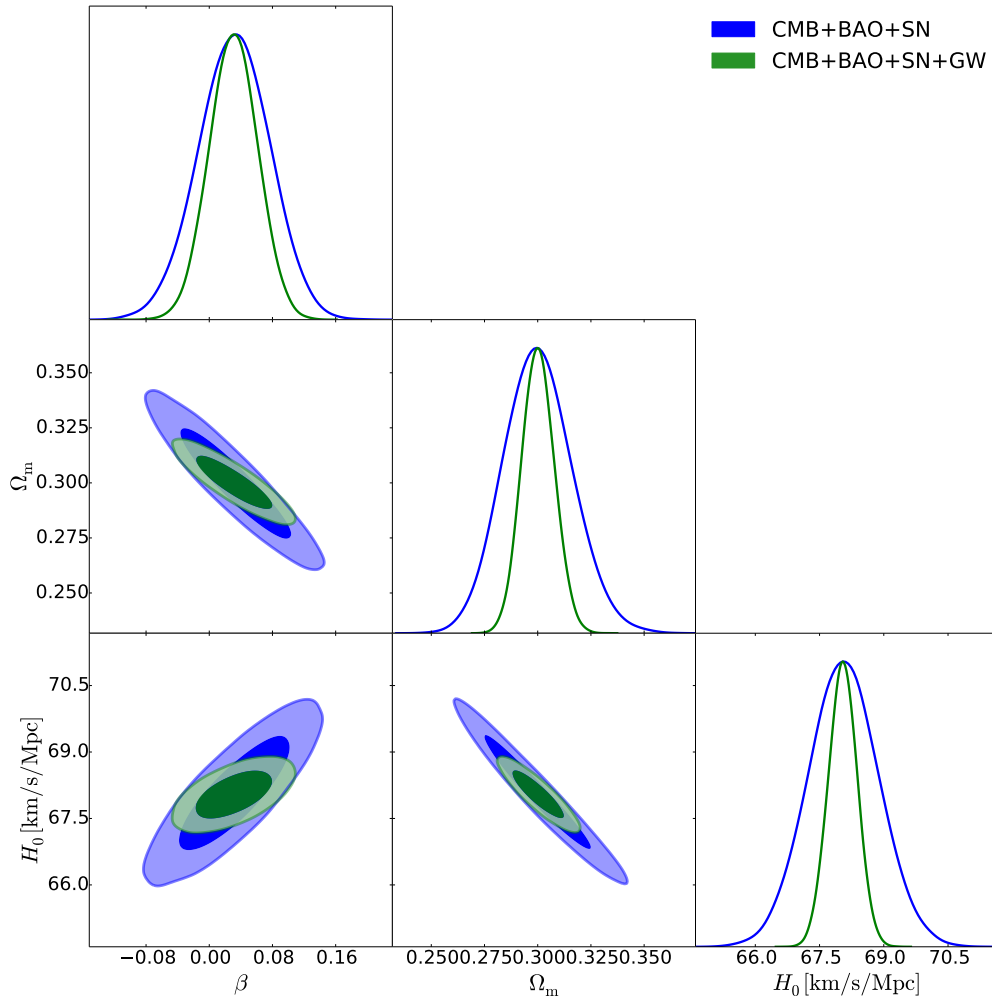


FIG. 2: Observational constraints (68.3% and 95.4% confidence level) on the IACDM2 model with $Q = \beta H_0 \rho_c$ by using the CMB+BAO+SN and CMB+BAO+SN+GW data.

TABLE III: Constraint errors for cosmological parameters of the IACDM models and the Iw CDM models using CBS and CBS+GW. Here, CBS stands for CMB+BAO+SN.

Model	IACDM1 ($Q = \beta H_0 \rho_c$)		IACDM2 ($Q = \beta H_0 \rho_c$)		Iw CDM1 ($Q = \beta H_0 \rho_c$)		Iw CDM2 ($Q = \beta H_0 \rho_c$)	
	CBS	CBS+GW	CBS	CBS+GW	CBS	CBS+GW	CBS	CBS+GW
$\sigma(\Omega_m)$	0.0081	0.0029	0.0160	0.0075	0.0082	0.0029	0.0265	0.0190
$\sigma(H_0 \text{ [km/s/Mpc]})$	0.6450	0.22	0.8	0.33	0.8350	0.18	0.82	0.4
$\sigma(\beta)$	0.0012	0.00088	0.044	0.03	0.0015	0.0013	0.093	0.078
$\sigma(w)$	—	—	—	—	0.04	0.026	0.0845	0.0683

TABLE IV: Constraint accuracies for cosmological parameters of the IACDM models and the Iw CDM models using CBS, and CBS+GW. Here, CBS stands for CMB+BAO+SN.

Model	IACDM1 ($Q = \beta H_0 \rho_c$)		IACDM2 ($Q = \beta H_0 \rho_c$)		Iw CDM1 ($Q = \beta H_0 \rho_c$)		Iw CDM2 ($Q = \beta H_0 \rho_c$)	
	CBS	CBS+GW	CBS	CBS+GW	CBS	CBS+GW	CBS	CBS+GW
$\varepsilon(\Omega_m)$	0.0266	0.0095	0.0533	0.0250	0.0267	0.0094	0.0798	0.0586
$\varepsilon(H_0 \text{ [km/s/Mpc]})$	0.0095	0.0032	0.0118	0.0049	0.0123	0.0026	0.0121	0.0059
$\varepsilon(w)$	—	—	—	—	0.0386	0.0251	0.0765	0.0635

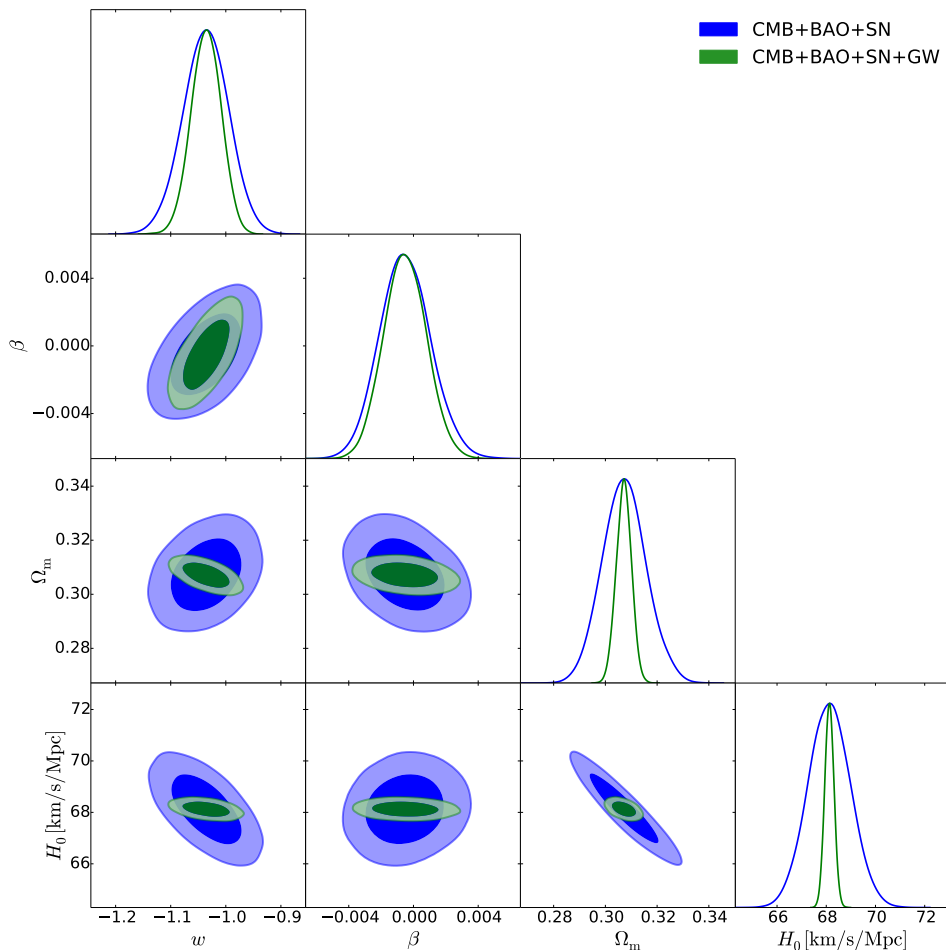


FIG. 3: Observational constraints (68.3% and 95.4% confidence level) on the $Iw\text{CDM1}$ model with $Q = \beta H_0 \rho_c$ by using the CMB+BAO+SN and CMB+BAO+SN+GW data.

reduced.

V. CONCLUSION

In this paper, we have investigated how the GW standard sirens impact the parameter estimation for the IDE models. We consider four various IDE models, i.e., the $I\Lambda\text{CDM1}$ ($Q = \beta H_0 \rho_c$) model, $I\Lambda\text{CDM2}$ ($Q = \beta H_0 \rho_c$) model, $Iw\text{CDM1}$ ($Q = \beta H_0 \rho_c$) model, and $Iw\text{CDM2}$ ($Q = \beta H_0 \rho_c$) respectively. The conventional optical observational data we used in this paper include, the Planck 2015 CMB data, the BAO measurements, and the SN data of Pantheon compilation. For the GW data, we simulated 1000 GW events based on the ET's ten-years observation. In order to quantify the constraint ability of the additional GW data, we consider two cases of data combination, namely CBS and CBS+GW, to constrain these models.

We find that the future GW standard sirens can significantly improve the constraints on most of the cosmological parameters for all the IDE models. When adding the

GW standard siren data, the constraint accuracy of H_0 can be remarkably improved, from 0.95%, 1.18%, 1.23%, 1.21% to the level of 0.32%, 0.49%, 0.26% and 0.59% for the $I\Lambda\text{CDM1}$, $I\Lambda\text{CDM2}$, $Iw\text{CDM1}$, and $Iw\text{CDM2}$ models, respectively. Moreover, as for the parameter Ω_m , the constraint accuracy was improved from 2.66%, 5.33%, 2.67%, 7.98% to 0.95%, 2.50%, 0.94% and 5.86%, for the four considered models separately. For the coupling constant β , when adding the GW data, the constraint absolute error $\sigma(\beta)$ can also be promoted, from 1.2×10^{-3} , 4.4×10^{-2} , 9.3×10^{-2} to 8.8×10^{-4} , 3.0×10^{-2} , and 7.8×10^{-2} for the $I\Lambda\text{CDM1}$, $I\Lambda\text{CDM2}$, and $Iw\text{CDM2}$ models respectively. While, in the $Iw\text{CDM1}$ model, the improvement is not conspicuous for this parameter, from $\sigma(\beta) = 1.5 \times 10^{-3}$ to $\sigma(\beta) = 1.3 \times 10^{-3}$. For the parameter w in the $Iw\text{CDM}$ models, the constraint accuracy could be improved as well when adding the GW data, i.e., from 3.86% to 2.51% for $Iw\text{CDM1}$ model and from 7.65% to 6.35% for $Iw\text{CDM2}$ model.

All in all, the precision of the parameter constraint can be promoted effectively with the consideration of future GW observation in the considered four IDE models. The

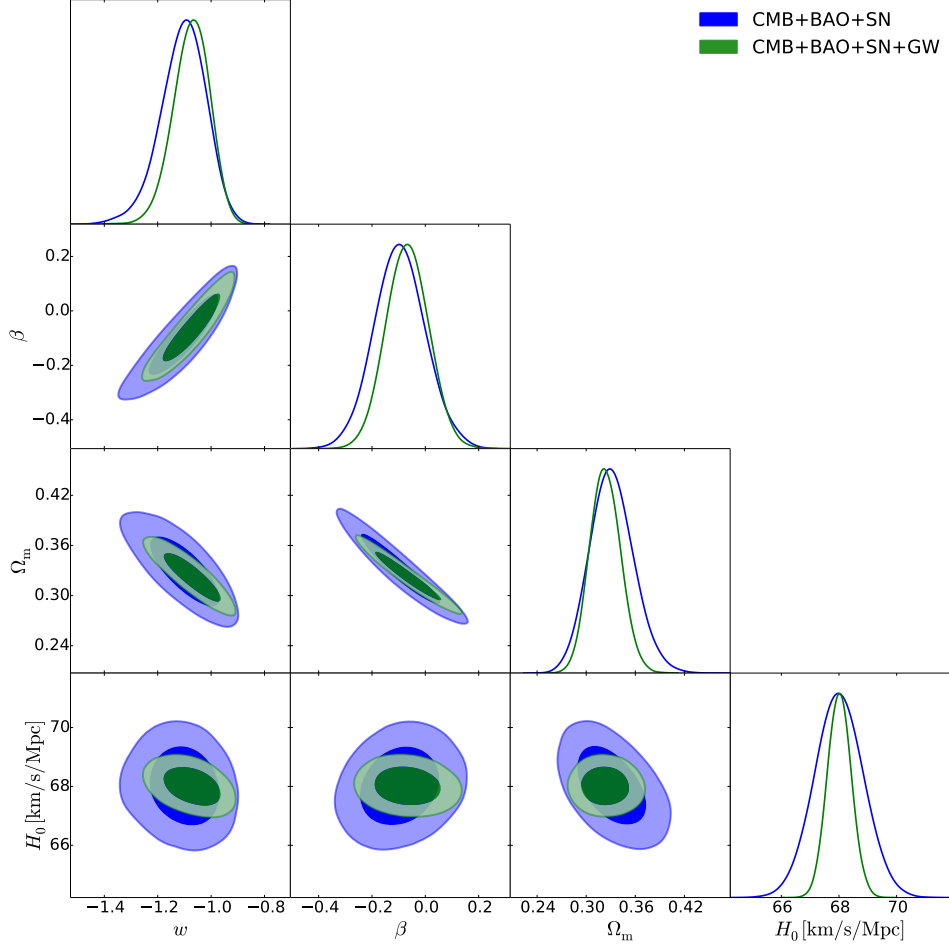


FIG. 4: Observational constraints (68.3% and 95.4% confidence level) on the $Iw\text{CDM}2$ model with $Q = \beta H_0 \rho_c$ by using the CMB+BAO+SN and CMB+BAO+SN+GW data.

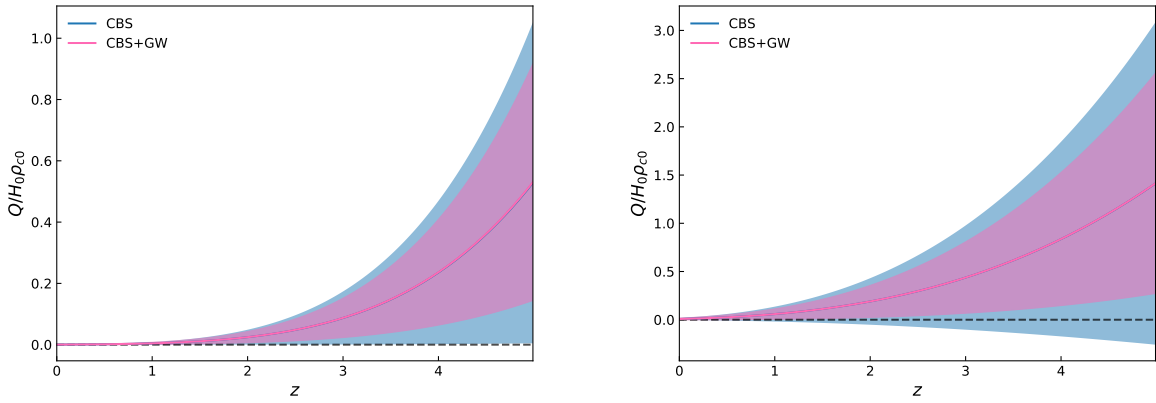


FIG. 5: The evolutions of $Q/H_0 \rho_{c0}$ (with 1σ errors) in the $Iw\text{CDM}1$ model with $Q = \beta H \rho_c$ (left) and in the $Iw\text{CDM}2$ model $Q = \beta H_0 \rho_c$ (right), respectively. The black dashed lines denote the noninteracting lines ($Q=0$).

results are consistent with the other extensively studied dark energy models. Thus, we can conclude that the improvement of the parameter constraint precision with future GW standard siren data may be independent of the cosmological models in the background. More DE and MG models should be explored to make this conclusion more reliable.

Acknowledgments

We would like to thank the anonymous referee for valu-

able suggestions that help us to improve this work significantly. We also thank Jing-Zhao Qi, Ze-Wei Zhao, and Ling-Feng Wang for helpful discussions. This work was supported by the National Natural Science Foundation of China (Grants Nos. 11875102, 11835009, 11690021, and 11522540) and the National Program for Support of Top-Notch Young Professionals.

-
- [1] A. G. Riess *et al.* [Supernova Search Team Collaboration], Observational evidence from supernovae for an accelerating universe and a cosmological constant, *Astron. J.* **116** (1998) 1009 [astro-ph/9805201].
- [2] S. Perlmutter *et al.* [Supernova Cosmology Project Collaboration], Measurements of Omega and Lambda from 42 high redshift supernovae, *Astrophys. J.* **517**, 565 (1999) [astro-ph/9812133].
- [3] D. N. Spergel *et al.* [WMAP Collaboration], First year Wilkinson Microwave Anisotropy Probe (WMAP) observations: Determination of cosmological parameters, *Astrophys. J. Suppl.* **148**, 175 (2003) [astro-ph/0302209].
- [4] C. L. Bennett *et al.* [WMAP Collaboration], First year Wilkinson Microwave Anisotropy Probe (WMAP) observations: Preliminary maps and basic results, *Astrophys. J. Suppl.* **148**, 1 (2003) [astro-ph/0302207].
- [5] M. Tegmark *et al.* [SDSS Collaboration], Cosmological parameters from SDSS and WMAP, *Phys. Rev. D* **69**, 103501 (2004) [astro-ph/0310723].
- [6] K. Abazajian *et al.* [SDSS Collaboration], The Second data release of the Sloan digital sky survey, *Astron. J.* **128**, 502 (2004) [astro-ph/0403325].
- [7] V. Sahni and A. Starobinsky, Reconstructing Dark Energy, *Int. J. Mod. Phys. D* **15**, 2105 (2006) [astro-ph/0610026].
- [8] K. Bamba, S. Capozziello, S. Nojiri and S. D. Odintsov, Dark energy cosmology: the equivalent description via different theoretical models and cosmography tests, *Astrophys. Space Sci.* **342**, 155 (2012) [arXiv:1205.3421 [gr-qc]].
- [9] S. Weinberg, The Cosmological Constant Problem, *Rev. Mod. Phys.* **61**, 1 (1989).
- [10] P. J. E. Peebles and B. Ratra, The Cosmological constant and dark energy, *Rev. Mod. Phys.* **75**, 559 (2003) [astro-ph/0207347].
- [11] E. J. Copeland, M. Sami and S. Tsujikawa, Dynamics of dark energy, *Int. J. Mod. Phys. D* **15**, 1753 (2006) [hep-th/0603057].
- [12] J. Frieman, M. Turner and D. Huterer, Dark Energy and the Accelerating Universe, *Ann. Rev. Astron. Astrophys.* **46**, 385 (2008) [arXiv:0803.0982 [astro-ph]].
- [13] V. Sahni, Reconstructing the properties of dark energy, *Prog. Theor. Phys. Suppl.* **172**, 110 (2008). doi:10.1143/PTPS.172.110
- [14] M. Li, X. D. Li, S. Wang and Y. Wang, Dark Energy, *Commun. Theor. Phys.* **56**, 525 (2011) [arXiv:1103.5870 [astro-ph.CO]].
- [15] M. Kamionkowski, Dark Matter and Dark Energy, arXiv:0706.2986 [astro-ph].
- [16] P. A. R. Ade *et al.* [Planck Collaboration], Planck 2015 results. XIII. Cosmological parameters, *Astron. Astrophys.* **594**, A13 (2016) [arXiv:1502.01589 [astro-ph.CO]].
- [17] V. Sahni and A. A. Starobinsky, The Case for a positive cosmological Lambda term, *Int. J. Mod. Phys. D* **9**, 373 (2000) [astro-ph/9904398].
- [18] R. Bean, S. M. Carroll and M. Trodden, Insights into dark energy: interplay between theory and observation, astro-ph/0510059.
- [19] L. Amendola, Coupled quintessence, *Phys. Rev. D* **62**, 043511 (2000) [astro-ph/9908023].
- [20] L. Amendola, Scaling solutions in general nonminimal coupling theories, *Phys. Rev. D* **60**, 043501 (1999) doi:10.1103/PhysRevD.60.043501 [astro-ph/9904120].
- [21] D. Tocchini-Valentini and L. Amendola, Stationary dark energy with a baryon dominated era: Solving the coincidence problem with a linear coupling, *Phys. Rev. D* **65**, 063508 (2002) doi:10.1103/PhysRevD.65.063508 [astro-ph/0108143].
- [22] L. Amendola and D. Tocchini-Valentini, Baryon bias and structure formation in an accelerating universe, *Phys. Rev. D* **66**, 043528 (2002) [astro-ph/0111535].
- [23] D. Comelli, M. Pietroni and A. Riotto, Dark energy and dark matter, *Phys. Lett. B* **571**, 115 (2003) doi:10.1016/j.physletb.2003.05.006 [hep-ph/0302080].
- [24] L. P. Chimento, A. S. Jakubi, D. Pavon and W. Zimdahl, Interacting quintessence solution to the coincidence problem, *Phys. Rev. D* **67**, 083513 (2003) doi:10.1103/PhysRevD.67.083513 [astro-ph/0303145].
- [25] R. G. Cai and A. Wang, Cosmology with interaction between phantom dark energy and dark matter and the coincidence problem, *JCAP* **0503**, 002 (2005) doi:10.1088/1475-7516/2005/03/002 [hep-th/0411025].
- [26] X. Zhang, F. Q. Wu and J. Zhang, New generalized Chaplygin gas as a scheme for unification of dark energy and dark matter, *JCAP* **0601**, 003 (2006) doi:10.1088/1475-7516/2006/01/003 [astro-ph/0411221].
- [27] F. Ferrer, S. Rasanen and J. Valiviita, Correlated isocurvature perturbations from mixed inflaton-curvaton decay, *JCAP* **0410**, 010 (2004) doi:10.1088/1475-

- 7516/2004/10/010 [astro-ph/0407300].
- [28] W. Zimdahl, Interacting dark energy and cosmological equations of state, *Int. J. Mod. Phys. D* **14**, 2319 (2005) doi:10.1142/S0218271805007784 [gr-qc/0505056].
- [29] X. Zhang, Statefinder diagnostic for coupled quintessence, *Phys. Lett. B* **611**, 1 (2005) doi:10.1016/j.physletb.2005.02.022 [astro-ph/0503075].
- [30] B. Wang, J. Zang, C. Y. Lin, E. Abdalla and S. Micheletti, Interacting dark energy and dark matter: observational constraints from cosmological parameters, *Nucl. Phys. B* **778**, 69 (2007) doi:10.1016/j.nuclphysb.2007.04.037 [astro-ph/0607126].
- [31] H. M. Sadjadi and M. Alimohammadi, Cosmological coincidence problem in interactive dark energy models, *Phys. Rev. D* **74**, 103007 (2006) doi:10.1103/PhysRevD.74.103007 [gr-qc/0610080].
- [32] J. D. Barrow and T. Clifton, Cosmologies with energy exchange, *Phys. Rev. D* **73**, 103520 (2006) doi:10.1103/PhysRevD.73.103520 [gr-qc/0604063].
- [33] M. Sasaki, J. Valiviita and D. Wands, Non-Gaussianity of the primordial perturbation in the curvaton model, *Phys. Rev. D* **74**, 103003 (2006) doi:10.1103/PhysRevD.74.103003 [astro-ph/0607627].
- [34] E. Abdalla, L. R. W. Abramo, L. Sodre, Jr. and B. Wang, Signature of the interaction between dark energy and dark matter in galaxy clusters, *Phys. Lett. B* **673**, 107 (2009) doi:10.1016/j.physletb.2009.02.008 [arXiv:0710.1198 [astro-ph]].
- [35] R. Bean, E. E. Flanagan and M. Trodden, Adiabatic instability in coupled dark energy-dark matter models, *Phys. Rev. D* **78**, 023009 (2008) doi:10.1103/PhysRevD.78.023009 [arXiv:0709.1128 [astro-ph]].
- [36] Z. K. Guo, N. Ohta and S. Tsujikawa, Probing the coupling between dark components of the universe, *Phys. Rev. D* **76**, 023508 (2007) doi:10.1103/PhysRevD.76.023508 [astro-ph/0702015 [astro-ph]].
- [37] O. Bertolami, F. Gil Pedro and M. Le Delliou, Dark energy-dark matter interaction and the violation of the equivalence principle from the Abell Cluster A586, *Phys. Lett. B* **654**, 165 (2007) doi:10.1016/j.physletb.2007.08.046 [astro-ph/0703462 [astro-ph]].
- [38] C. G. Boehmer, G. Caldera-Cabral, R. Lazkoz and R. Maartens, Dynamics of dark energy with a coupling to dark matter, *Phys. Rev. D* **78**, 023505 (2008) doi:10.1103/PhysRevD.78.023505 [arXiv:0801.1565 [gr-qc]].
- [39] J. H. He and B. Wang, Effects of the interaction between dark energy and dark matter on cosmological parameters, *JCAP* **0806**, 010 (2008) doi:10.1088/1475-7516/2008/06/010 [arXiv:0801.4233 [astro-ph]].
- [40] G. Caldera-Cabral, R. Maartens and L. A. Urena-Lopez, Dynamics of interacting dark energy, *Phys. Rev. D* **79**, 063518 (2009) doi:10.1103/PhysRevD.79.063518 [arXiv:0812.1827 [gr-qc]].
- [41] R. Bean, E. E. Flanagan, I. Laszlo and M. Trodden, Constraining Interactions in Cosmology's Dark Sector, *Phys. Rev. D* **78**, 123514 (2008) doi:10.1103/PhysRevD.78.123514 [arXiv:0808.1105 [astro-ph]].
- [42] M. Szydlowski, A. Krawiec, A. Kurek and M. Kamionka, AIC, BIC, Bayesian evidence against the interacting dark energy model, *Eur. Phys. J. C* **75**, no. 99, 5 (2015) doi:10.1140/epjc/s10052-014-3236-1 [arXiv:0801.0638 [astro-ph]].
- [43] X. m. Chen, Y. g. Gong and E. N. Saridakis, Phase-space analysis of interacting phantom cosmology, *JCAP* **0904**, 001 (2009) doi:10.1088/1475-7516/2009/04/001 [arXiv:0812.1117 [gr-qc]].
- [44] J. Valiviita, E. Majerotto and R. Maartens, Instability in interacting dark energy and dark matter fluids, *JCAP* **0807**, 020 (2008) doi:10.1088/1475-7516/2008/07/020 [arXiv:0804.0232 [astro-ph]].
- [45] E. Couderc and S. Klein, Coherent rho0 photoproduction in bulk matter at high energies, *Phys. Rev. Lett.* **103**, 062504 (2009) doi:10.1103/PhysRevLett.103.062504 [arXiv:0901.1161 [nucl-th]].
- [46] L. P. Chimento, Linear and nonlinear interactions in the dark sector, *Phys. Rev. D* **81**, 043525 (2010) doi:10.1103/PhysRevD.81.043525 [arXiv:0911.5687 [astro-ph.CO]].
- [47] G. Caldera-Cabral, R. Maartens and B. M. Schaefer, The Growth of Structure in Interacting Dark Energy Models, *JCAP* **0907**, 027 (2009) doi:10.1088/1475-7516/2009/07/027 [arXiv:0905.0492 [astro-ph.CO]].
- [48] E. Majerotto, J. Valiviita and R. Maartens, Adiabatic initial conditions for perturbations in interacting dark energy models, *Mon. Not. Roy. Astron. Soc.* **402**, 2344 (2010) doi:10.1111/j.1365-2966.2009.16140.x [arXiv:0907.4981 [astro-ph.CO]].
- [49] J. Valiviita, R. Maartens and E. Majerotto, Observational constraints on an interacting dark energy model, *Mon. Not. Roy. Astron. Soc.* **402**, 2355 (2010) doi:10.1111/j.1365-2966.2009.16115.x [arXiv:0907.4987 [astro-ph.CO]].
- [50] J. H. He, B. Wang and Y. P. Jing, Effects of dark sectors' mutual interaction on the growth of structures, *JCAP* **0907**, 030 (2009) doi:10.1088/1475-7516/2009/07/030 [arXiv:0902.0660 [gr-qc]].
- [51] J. H. He, B. Wang and P. Zhang, The imprint of the interaction between dark sectors in large scale cosmic microwave background anisotropies, *Phys. Rev. D* **80**, 063530 (2009) doi:10.1103/PhysRevD.80.063530 [arXiv:0906.0677 [gr-qc]].
- [52] K. Koyama, R. Maartens and Y. S. Song, Velocities as a probe of dark sector interactions, *JCAP* **0910**, 017 (2009) doi:10.1088/1475-7516/2009/10/017 [arXiv:0907.2126 [astro-ph.CO]].
- [53] M. Li, X. D. Li, S. Wang, Y. Wang and X. Zhang, Probing interaction and spatial curvature in the holographic dark energy model, *JCAP* **0912**, 014 (2009) doi:10.1088/1475-7516/2009/12/014 [arXiv:0910.3855 [astro-ph.CO]].
- [54] J. Q. Xia, Constraint on coupled dark energy models from observations, *Phys. Rev. D* **80**, 103514 (2009) doi:10.1103/PhysRevD.80.103514 [arXiv:0911.4820 [astro-ph.CO]].
- [55] R. G. Cai and Q. Su, On the Dark Sector Interactions, *Phys. Rev. D* **81**, 103514 (2010) doi:10.1103/PhysRevD.81.103514 [arXiv:0912.1943 [astro-ph.CO]].
- [56] J. H. He, B. Wang, E. Abdalla and D. Pavon, The Imprint of the interaction between dark sectors in galaxy clusters, *JCAP* **1012**, 022 (2010) doi:10.1088/1475-

- 7516/2010/12/022 [arXiv:1001.0079 [gr-qc]].
- [57] J. Cui and X. Zhang, Cosmic age problem revisited in the holographic dark energy model, *Phys. Lett. B* **690**, 233 (2010) doi:10.1016/j.physletb.2010.05.046 [arXiv:1005.3587 [astro-ph.CO]].
- [58] B. Li and J. D. Barrow, On the Effects of Coupled Scalar Fields on Structure Formation, *Mon. Not. Roy. Astron. Soc.* **413**, 262 (2011) doi:10.1111/j.1365-2966.2010.18130.x [arXiv:1010.3748 [astro-ph.CO]].
- [59] M. B. Gavela, L. Lopez Honorez, O. Mena and S. Rigolin, Dark Coupling and Gauge Invariance, *JCAP* **1011**, 044 (2010) doi:10.1088/1475-7516/2010/11/044 [arXiv:1005.0295 [astro-ph.CO]].
- [60] M. Martinelli, L. Lopez Honorez, A. Melchiorri and O. Mena, Future CMB cosmological constraints in a dark coupled universe, *Phys. Rev. D* **81**, 103534 (2010) doi:10.1103/PhysRevD.81.103534 [arXiv:1004.2410 [astro-ph.CO]].
- [61] J. H. He, B. Wang and E. Abdalla, Testing the interaction between dark energy and dark matter via latest observations, *Phys. Rev. D* **83**, 063515 (2011) doi:10.1103/PhysRevD.83.063515 [arXiv:1012.3904 [astro-ph.CO]].
- [62] Y. Chen, Z. H. Zhu, L. Xu and J. S. Alcaniz, $\Lambda(t)$ CDM Model as a Unified Origin of Holographic and Agegraphic Dark Energy Models, *Phys. Lett. B* **698**, 175 (2011) doi:10.1016/j.physletb.2011.02.052 [arXiv:1103.2512 [astro-ph.CO]].
- [63] T. F. Fu, J. F. Zhang, J. Q. Chen and X. Zhang, Holographic Ricci dark energy: Interacting model and cosmological constraints, *Eur. Phys. J. C* **72**, 1932 (2012) doi:10.1140/epjc/s10052-012-1932-2 [arXiv:1112.2350 [astro-ph.CO]].
- [64] T. Clemson, K. Koyama, G. B. Zhao, R. Maartens and J. Valiviita, Interacting Dark Energy – constraints and degeneracies, *Phys. Rev. D* **85**, 043007 (2012) doi:10.1103/PhysRevD.85.043007 [arXiv:1109.6234 [astro-ph.CO]].
- [65] Y. H. Li and X. Zhang, Running coupling: Does the coupling between dark energy and dark matter change sign during the cosmological evolution?, *Eur. Phys. J. C* **71**, 1700 (2011) doi:10.1140/epjc/s10052-011-1700-8 [arXiv:1103.3185 [astro-ph.CO]].
- [66] X. D. Xu and B. Wang, Breaking parameter degeneracy in interacting dark energy models from observations, *Phys. Lett. B* **701**, 513 (2011) doi:10.1016/j.physletb.2011.06.043 [arXiv:1103.2632 [astro-ph.CO]].
- [67] Z. Zhang, S. Li, X. D. Li, X. Zhang and M. Li, Revisit of the Interaction between Holographic Dark Energy and Dark Matter, *JCAP* **1206**, 009 (2012) doi:10.1088/1475-7516/2012/06/009 [arXiv:1204.6135 [astro-ph.CO]].
- [68] X. D. Xu, B. Wang, P. Zhang and F. Atrio-Barandela, The effect of Dark Matter and Dark Energy interactions on the peculiar velocity field and the kinetic Sunyaev-Zel'dovich effect, *JCAP* **1312**, 001 (2013) doi:10.1088/1475-7516/2013/12/001 [arXiv:1308.1475 [astro-ph.CO]].
- [69] M. J. Zhang and W. B. Liu, Observational constraint on the interacting dark energy models including the Sandage-Loeb test, *Eur. Phys. J. C* **74**, 2863 (2014) doi:10.1140/epjc/s10052-014-2863-x [arXiv:1312.0224 [astro-ph.CO]].
- [70] Y. Wang, D. Wands, L. Xu, J. De-Santiago and A. Hojjati, Cosmological constraints on a decomposed Chaplygin gas, *Phys. Rev. D* **87**, no. 8, 083503 (2013) doi:10.1103/PhysRevD.87.083503 [arXiv:1301.5315 [astro-ph.CO]].
- [71] V. Salvatelli, A. Marchini, L. Lopez-Honorez and O. Mena, New constraints on Coupled Dark Energy from the Planck satellite experiment, *Phys. Rev. D* **88**, no. 2, 023531 (2013) doi:10.1103/PhysRevD.88.023531 [arXiv:1304.7119 [astro-ph.CO]].
- [72] W. Yang and L. Xu, Cosmological constraints on interacting dark energy with redshift-space distortion after Planck data, *Phys. Rev. D* **89**, no. 8, 083517 (2014) doi:10.1103/PhysRevD.89.083517 [arXiv:1401.1286 [astro-ph.CO]].
- [73] W. Yang and L. Xu, Testing coupled dark energy with large scale structure observation, *JCAP* **1408**, 034 (2014) doi:10.1088/1475-7516/2014/08/034 [arXiv:1401.5177 [astro-ph.CO]].
- [74] S. Wang, Y. Z. Wang, J. J. Geng and X. Zhang, Effects of time-varying β in SNLS3 on constraining interacting dark energy models, *Eur. Phys. J. C* **74**, no. 11, 3148 (2014) doi:10.1140/epjc/s10052-014-3148-0 [arXiv:1406.0072 [astro-ph.CO]].
- [75] V. Faraoni, J. B. Dent and E. N. Saridakis, Covariantizing the interaction between dark energy and dark matter, *Phys. Rev. D* **90**, no. 6, 063510 (2014) doi:10.1103/PhysRevD.90.063510 [arXiv:1405.7288 [gr-qc]].
- [76] J. L. Cui, L. Yin, L. F. Wang, Y. H. Li and X. Zhang, A closer look at interacting dark energy with statefinder hierarchy and growth rate of structure, *JCAP* **1509**, no. 09, 024 (2015) doi:10.1088/1475-7516/2015/09/024 [arXiv:1503.08948 [astro-ph.CO]].
- [77] Y. Fan, P. Wu and H. Yu, Cosmological perturbations of non-minimally coupled quintessence in the metric and Palatini formalisms, *Phys. Lett. B* **746**, 230 (2015). doi:10.1016/j.physletb.2015.05.005
- [78] T. Yang, Z. K. Guo and R. G. Cai, Reconstructing the interaction between dark energy and dark matter using Gaussian Processes, *Phys. Rev. D* **91**, no. 12, 123533 (2015) doi:10.1103/PhysRevD.91.123533 [arXiv:1505.04443 [astro-ph.CO]].
- [79] D. G. A. Duniya, D. Bertacca and R. Maartens, Probing the imprint of interacting dark energy on very large scales, *Phys. Rev. D* **91**, 063530 (2015) doi:10.1103/PhysRevD.91.063530 [arXiv:1502.06424 [astro-ph.CO]].
- [80] L. Feng and X. Zhang, Revisit of the interacting holographic dark energy model after Planck 2015, *JCAP* **1608**, no. 08, 072 (2016) doi:10.1088/1475-7516/2016/08/072 [arXiv:1607.05567 [astro-ph.CO]].
- [81] R. Murgia, S. Gariazzo and N. Fornengo, Constraints on the coupling between dark energy and dark matter from CMB data, *JCAP* **1604**, no. 04, 014 (2016) doi:10.1088/1475-7516/2016/04/014 [arXiv:1602.01765 [astro-ph.CO]].
- [82] J. Sol, A. Gmez-Valent and J. de Cruz Prez, *Astrophys. J.* **836**, no. 1, 43 (2017) doi:10.3847/1538-4357/836/1/43 [arXiv:1602.02103 [astro-ph.CO]].
- [83] J. Sol Peracaula, J. de Cruz Prez and A. Gmez-Valent, Dynamical dark energy vs. $\Lambda = \text{const}$ in light of observations, *EPL* **121**, no. 3, 39001 (2018) doi:10.1209/0295-5075/121/39001 [arXiv:1606.00450 [gr-qc]].

- [84] J. Sola, Cosmological constant vis-a-vis dynamical vacuum: bold challenging the Λ CDM, *Int. J. Mod. Phys. A* **31**, no. 23, 1630035 (2016) doi:10.1142/S0217751X16300350 [arXiv:1612.02449 [astro-ph.CO]].
- [85] A. Pourtsidou and T. Tram, Reconciling CMB and structure growth measurements with dark energy interactions, *Phys. Rev. D* **94**, no. 4, 043518 (2016) doi:10.1103/PhysRevD.94.043518 [arXiv:1604.04222 [astro-ph.CO]].
- [86] A. A. Costa, X. D. Xu, B. Wang and E. Abdalla, Constraints on interacting dark energy models from Planck 2015 and redshift-space distortion data, *JCAP* **1701**, no. 01, 028 (2017) doi:10.1088/1475-7516/2017/01/028 [arXiv:1605.04138 [astro-ph.CO]].
- [87] D. M. Xia and S. Wang, Constraining interacting dark energy models with latest cosmological observations, *Mon. Not. Roy. Astron. Soc.* **463**, 952 (2016) doi:10.1093/mnras/stw2073 [arXiv:1608.04545 [astro-ph.CO]].
- [88] C. van de Bruck, J. Mifsud and J. Morrice, Testing coupled dark energy models with their cosmological background evolution, *Phys. Rev. D* **95**, no. 4, 043513 (2017) doi:10.1103/PhysRevD.95.043513 [arXiv:1609.09855 [astro-ph.CO]].
- [89] S. Kumar and R. C. Nunes, Probing the interaction between dark matter and dark energy in the presence of massive neutrinos, *Phys. Rev. D* **94**, no. 12, 123511 (2016) doi:10.1103/PhysRevD.94.123511 [arXiv:1608.02454 [astro-ph.CO]].
- [90] S. Kumar and R. C. Nunes, Echo of interactions in the dark sector, *Phys. Rev. D* **96**, no. 10, 103511 (2017) doi:10.1103/PhysRevD.96.103511 [arXiv:1702.02143 [astro-ph.CO]].
- [91] L. Santos, W. Zhao, E. G. M. Ferreira and J. Quintin, Constraining interacting dark energy with CMB and BAO future surveys, *Phys. Rev. D* **96**, no. 10, 103529 (2017) doi:10.1103/PhysRevD.96.103529 [arXiv:1707.06827 [astro-ph.CO]].
- [92] J. Sol Peracaula, J. d. C. Perez and A. Gomez-Valent, Possible signals of vacuum dynamics in the Universe, *Mon. Not. Roy. Astron. Soc.* **478**, no. 4, 4357 (2018) doi:10.1093/mnras/sty1253 [arXiv:1703.08218 [astro-ph.CO]].
- [93] R. Y. Guo, Y. H. Li, J. F. Zhang and X. Zhang, Weighing neutrinos in the scenario of vacuum energy interacting with cold dark matter: application of the parameterized post-Friedmann approach, *JCAP* **1705**, no. 05, 040 (2017) doi:10.1088/1475-7516/2017/05/040 [arXiv:1702.04189 [astro-ph.CO]].
- [94] X. Zhang, Probing the interaction between dark energy and dark matter with the parameterized post-Friedmann approach, *Sci. China Phys. Mech. Astron.* **60**, no. 5, 050431 (2017) doi:10.1007/s11433-017-9013-7 [arXiv:1702.04564 [astro-ph.CO]].
- [95] L. Feng, Y. H. Li, F. Yu, J. F. Zhang and X. Zhang, Exploring interacting holographic dark energy in a perturbed universe with parameterized post-Friedmann approach, *Eur. Phys. J. C* **78**, no. 10, 865 (2018) doi:10.1140/epjc/s10052-018-6338-3 [arXiv:1807.03022 [astro-ph.CO]].
- [96] M. M. Zhao, R. Y. Guo, J. F. Zhang and X. Zhang, Dark energy versus modified gravity: Impacts on measuring neutrino mass, arXiv:1810.11658 [astro-ph.CO].
- [97] W. Yang, S. Pan, E. Di Valentino, R. C. Nunes, S. Vagnozzi and D. F. Mota, Tale of stable interacting dark energy, observational signatures, and the H_0 tension, *JCAP* **1809**, no. 09, 019 (2018) doi:10.1088/1475-7516/2018/09/019 [arXiv:1805.08252 [astro-ph.CO]].
- [98] C. Li, X. Ren, M. Khurshudyan and Y. F. Cai, Implications of the possible 21-cm line excess at cosmic dawn on dynamics of interacting dark energy, arXiv:1904.02458 [astro-ph.CO].
- [99] A. A. Costa, X. D. Xu, B. Wang, E. G. M. Ferreira and E. Abdalla, Testing the Interaction between Dark Energy and Dark Matter with Planck Data, *Phys. Rev. D* **89**, no. 10, 103531 (2014) doi:10.1103/PhysRevD.89.103531 [arXiv:1311.7380 [astro-ph.CO]].
- [100] V. Salvatelli, N. Said, M. Bruni, A. Melchiorri and D. Wands, Indications of a late-time interaction in the dark sector, *Phys. Rev. Lett.* **113**, no. 18, 181301 (2014) doi:10.1103/PhysRevLett.113.181301 [arXiv:1406.7297 [astro-ph.CO]].
- [101] R. C. Nunes, S. Pan and E. N. Saridakis, New constraints on interacting dark energy from cosmic chronometers, *Phys. Rev. D* **94**, no. 2, 023508 (2016) doi:10.1103/PhysRevD.94.023508 [arXiv:1605.01712 [astro-ph.CO]].
- [102] E. G. M. Ferreira, J. Quintin, A. A. Costa, E. Abdalla and B. Wang, Evidence for interacting dark energy from BOSS, *Phys. Rev. D* **95**, no. 4, 043520 (2017) doi:10.1103/PhysRevD.95.043520 [arXiv:1412.2777 [astro-ph.CO]].
- [103] W. Yang, S. Pan and D. F. Mota, Novel approach toward the large-scale stable interacting dark-energy models and their astronomical bounds, *Phys. Rev. D* **96**, no. 12, 123508 (2017) doi:10.1103/PhysRevD.96.123508 [arXiv:1709.00006 [astro-ph.CO]].
- [104] W. Yang, S. Pan and J. D. Barrow, Large-scale Stability and Astronomical Constraints for Coupled Dark-Energy Models, *Phys. Rev. D* **97**, no. 4, 043529 (2018) doi:10.1103/PhysRevD.97.043529 [arXiv:1706.04953 [astro-ph.CO]].
- [105] H. L. Li, L. Feng, J. F. Zhang and X. Zhang, Models of vacuum energy interacting with cold dark matter: Constraints and comparison, *Sci. China Phys. Mech. Astron.* **62**, no. 12, 120411 (2019) doi:10.1007/s11433-019-9439-8 [arXiv:1812.00319 [astro-ph.CO]].
- [106] L. Feng, H. L. Li, J. F. Zhang and X. Zhang, Exploring neutrino mass and mass hierarchy in interacting dark energy models, arXiv:1903.08848 [astro-ph.CO].
- [107] R. Y. Guo, J. F. Zhang and X. Zhang, Can the H_0 tension be resolved in extensions to Λ CDM cosmology?, *JCAP* **1902**, 054 (2019) doi:10.1088/1475-7516/2019/02/054 [arXiv:1809.02340 [astro-ph.CO]].
- [108] A. A. Costa, R. C. G. Landim, B. Wang and E. Abdalla, Interacting Dark Energy: Possible Explanation for 21-cm Absorption at Cosmic Dawn, *Eur. Phys. J. C* **78**, no. 9, 746 (2018) doi:10.1140/epjc/s10052-018-6237-7 [arXiv:1803.06944 [astro-ph.CO]].
- [109] L. Xiao, R. An, L. Zhang, B. Yue, Y. Xu and B. Wang, Can conformal and disformal couplings between dark sectors explain the EDGES 21-cm anomaly?, *Phys. Rev. D* **99**, no. 2, 023528 (2019) doi:10.1103/PhysRevD.99.023528 [arXiv:1807.05541 [astro-ph.CO]].
- [110] B. F. Schutz, *Nature* **323**, 310 (1986).

- doi:10.1038/323310a0
- [111] D. E. Holz and S. A. Hughes, *Astrophys. J.* **629**, 15 (2005) doi:10.1086/431341 [astro-ph/0504616].
- [112] B. P. Abbott *et al.* [LIGO Scientific and Virgo and 1M2H and Dark Energy Camera GW-E and DES and DLT40 and Las Cumbres Observatory and VINROUGE and MASTER Collaborations], *Nature* **551**, no. 7678, 85 (2017) doi:10.1038/nature24471 [arXiv:1710.05835 [astro-ph.CO]].
- [113] Einstein gravitational wave Telescope conceptual design study, <http://www.et-gw.eu/et/>.
- [114] X. N. Zhang, L. F. Wang, J. F. Zhang and X. Zhang, Improving cosmological parameter estimation with the future gravitational-wave standard siren observation from the Einstein Telescope, *Phys. Rev. D* **99**, no. 6, 063510 (2019) doi:10.1103/PhysRevD.99.063510 [arXiv:1804.08379 [astro-ph.CO]].
- [115] W. Zhao, B. S. Wright and B. Li, Constraining the time variation of Newton's constant G with gravitational-wave standard sirens and supernovae, *JCAP* **1810**, no. 10, 052 (2018) doi:10.1088/1475-7516/2018/10/052 [arXiv:1804.03066 [astro-ph.CO]].
- [116] M. Du, W. Yang, L. Xu, S. Pan and D. F. Mota, Future Constraints on Dynamical Dark-Energy using Gravitational-Wave Standard Sirens, arXiv:1812.01440 [astro-ph.CO].
- [117] J. F. Zhang, H. Y. Dong, J. Z. Qi and X. Zhang, Prospect for constraining holographic dark energy with gravitational wave standard sirens from the Einstein Telescope, arXiv:1906.07504 [astro-ph.CO].
- [118] W. Yang, S. Pan, E. Di Valentino, B. Wang and A. Wang, Forecasting Interacting Vacuum-Energy Models using Gravitational Waves, arXiv:1904.11980 [astro-ph.CO].
- [119] W. Yang, S. Vagnozzi, E. Di Valentino, R. C. Nunes, S. Pan and D. F. Mota, Listening to the sound of dark sector interactions with gravitational wave standard sirens, arXiv:1905.08286 [astro-ph.CO].
- [120] R. R. A. Bachega, E. Abdalla and K. S. F. Fornazier, Forecasting the Interaction in Dark Matter-Dark Energy Models with Standard Sirens From the Einstein Telescope, arXiv:1906.08909 [astro-ph.CO].
- [121] J. F. Zhang, M. Zhang, S. J. Jin, J. Z. Qi and X. Zhang, Cosmological parameter estimation with future gravitational wave standard siren observation from the Einstein Telescope, arXiv:1907.03238 [astro-ph.CO].
- [122] X. Zhang, Gravitational wave standard sirens and cosmological parameter measurement, arXiv:1905.11122 [astro-ph.CO].
- [123] Z. Chang, Q. G. Huang, S. Wang and Z. C. Zhao, Low-redshift constraints on the Hubble constant from the baryon acoustic oscillation standard rulers and the gravitational wave standard sirens, *Eur. Phys. J. C* **79**, no. 2, 177 (2019). doi:10.1140/epjc/s10052-019-6664-0
- [124] J. h. He, Accurate method to determine the systematics due to the peculiar velocities of galaxies in measuring the Hubble constant from gravitational-wave standard sirens, *Phys. Rev. D* **100**, no. 2, 023527 (2019) doi:10.1103/PhysRevD.100.023527 [arXiv:1903.11254 [astro-ph.CO]].
- [125] Y. H. Li, J. F. Zhang and X. Zhang, Parametrized Post-Friedmann Framework for Interacting Dark Energy, *Phys. Rev. D* **90**, no. 6, 063005 (2014) doi:10.1103/PhysRevD.90.063005 [arXiv:1404.5220 [astro-ph.CO]].
- [126] W. Hu, Parametrized Post-Friedmann Signatures of Acceleration in the CMB, *Phys. Rev. D* **77**, 103524 (2008) doi:10.1103/PhysRevD.77.103524 [arXiv:0801.2433 [astro-ph]].
- [127] W. Fang, W. Hu and A. Lewis, Crossing the Phantom Divide with Parameterized Post-Friedmann Dark Energy, *Phys. Rev. D* **78**, 087303 (2008) doi:10.1103/PhysRevD.78.087303 [arXiv:0808.3125 [astro-ph]].
- [128] N. Aghanim *et al.* [Planck Collaboration], Planck 2015 results. XI. CMB power spectra, likelihoods, and robustness of parameters, *Astron. Astrophys.* **594**, A11 (2016) doi:10.1051/0004-6361/201526926 [arXiv:1507.02704 [astro-ph.CO]].
- [129] F. Beutler *et al.*, The 6dF Galaxy Survey: Baryon Acoustic Oscillations and the Local Hubble Constant, *Mon. Not. Roy. Astron. Soc.* **416**, 3017 (2011) doi:10.1111/j.1365-2966.2011.19250.x [arXiv:1106.3366 [astro-ph.CO]].
- [130] A. J. Ross, L. Samushia, C. Howlett, W. J. Percival, A. Burden and M. Manera, The clustering of the SDSS DR7 main Galaxy sample C I. A 4 per cent distance measure at $z = 0.15$, *Mon. Not. Roy. Astron. Soc.* **449**, no. 1, 835 (2015) doi:10.1093/mnras/stv154 [arXiv:1409.3242 [astro-ph.CO]].
- [131] S. Alam *et al.* [BOSS Collaboration], The clustering of galaxies in the completed SDSS-III Baryon Oscillation Spectroscopic Survey: cosmological analysis of the DR12 galaxy sample, *Mon. Not. Roy. Astron. Soc.* **470**, no. 3, 2617 (2017) doi:10.1093/mnras/stx721 [arXiv:1607.03155 [astro-ph.CO]].
- [132] D. M. Scolnic *et al.*, The Complete Light-curve Sample of Spectroscopically Confirmed SNe Ia from Pan-STARRS1 and Cosmological Constraints from the Combined Pantheon Sample, *Astrophys. J.* **859**, no. 2, 101 (2018) doi:10.3847/1538-4357/aab9bb [arXiv:1710.00845 [astro-ph.CO]].
- [133] L. F. Wang, X. N. Zhang, J. F. Zhang and X. Zhang, Impacts of gravitational-wave standard siren observation of the Einstein Telescope on weighing neutrinos in cosmology, *Phys. Lett. B* **782**, 87 (2018) doi:10.1016/j.physletb.2018.05.027 [arXiv:1802.04720 [astro-ph.CO]].
- [134] W. Zhao, C. Van Den Broeck, D. Baskaran and T. G. F. Li, Determination of Dark Energy by the Einstein Telescope: Comparing with CMB, BAO and SNIa Observations, *Phys. Rev. D* **83**, 023005 (2011) doi:10.1103/PhysRevD.83.023005 [arXiv:1009.0206 [astro-ph.CO]].
- [135] R. G. Cai and T. Yang, Estimating cosmological parameters by the simulated data of gravitational waves from the Einstein Telescope, *Phys. Rev. D* **95**, no. 4, 044024 (2017) doi:10.1103/PhysRevD.95.044024 [arXiv:1608.08008 [astro-ph.CO]].
- [136] J. Abadie *et al.* [LIGO Scientific Collaboration], Calibration of the LIGO Gravitational Wave Detectors in the Fifth Science Run, *Nucl. Instrum. Meth. A* **624**, 223 (2010) doi:10.1016/j.nima.2010.07.089 [arXiv:1007.3973 [gr-qc]].
- [137] R. Schneider, V. Ferrari, S. Matarrese and S. F. Portegies Zwart, Gravitational waves from cosmological compact binaries, *Mon. Not. Roy. Astron. Soc.* **324**, 797 (2001) doi:10.1046/j.1365-8711.2001.04217.x [astro-ph.CO].

- ph/0002055].
- [138] C. Cutler and D. E. Holz, Ultra-high precision cosmology from gravitational waves, *Phys. Rev. D* **80**, 104009 (2009) doi:10.1103/PhysRevD.80.104009 [arXiv:0906.3752 [astro-ph.CO]].